

**THE INTERNATIONAL RESEARCH GROUP ON WOOD PRESERVATION**

**Section**

**Biology**

**The use of X-ray diffraction for analyzing biomodification of  
crystalline cellulose by wood decay fungi**

Caitlin Howell<sup>1\*</sup>, Anne Christine Steenkjær Hastrup<sup>2</sup> and Jody Jellison<sup>1</sup>

Department of Biological Sciences  
University of Maine  
311 Hitchner Hall, Orono, Maine, 04469  
USA

Department of Microbiology  
University of Copenhagen  
Sølvgade 83H, 1307 Copenhagen K  
Denmark

\*Corresponding author. Tel: +1-207-581-3032; Email: [caitlin.howell@umit.maine.edu](mailto:caitlin.howell@umit.maine.edu)

Paper prepared for the 38<sup>th</sup> Annual Meeting  
Jackson Lake Lodge, Wyoming, USA  
20-24 May, 2007

**IRG SECRETARIAT**  
**SE-100 44 Stockholm**  
**Sweden**  
[www.irg-wp.com](http://www.irg-wp.com)

# The use of X-ray diffraction for analyzing biomodification of crystalline cellulose by wood decay fungi

Caitlin Howell<sup>1\*</sup>, Anne Christine Steenkjær Hastrup<sup>2</sup> and Jody Jellison<sup>1</sup>

<sup>1</sup> Department of Biological Sciences, University of Maine  
311 Hitchner Hall, Orono, Maine, 04469, USA

<sup>2</sup> Department of Microbiology, University of Copenhagen, Sølvgade 83H, 1307 Copenhagen K, Denmark

\*Corresponding author. Tel: +1-207-581-3032; Email: caitlin.howell@umit.maine.edu

## ABSTRACT

X-ray diffraction (XRD) is based on the creation of an interference pattern by x-rays when they encounter a regularly spaced matrix. In wood, this process has been used to determine among other things the average width of the cellulose microcrystals, the percent of crystalline cellulose within the wood, and can be used to examine the changes in these parameters during degradation. Enhanced understanding of the mechanisms and effects of wood degradation through x-ray diffraction may improve knowledge of degradative processes and facilitate the development of more effective decay prevention measures.

Studies were conducted to determine changes over time in wood crystallinity generated by the brown rot fungus *Meruliporia incrassata* and the soft rot fungus *Chaetomium elatum*. Fungi were grown in modified soil block jars with spruce wood blocks for 2, 4, 6 and 8 weeks. After removal from the jars, wood blocks were dried, analyzed for weight loss, ground into powder and pressed into pellets. Pellets were analyzed by x-ray diffraction using a  $\theta$ - $2\theta$  scan and the resulting spectra were deconvoluted to determine average crystallite width and overall percent crystallinity.

Results showed an increase in crystallite width by *M. incrassata* by the fourth week of decay, followed by a slow decrease. Percent crystallinity values showed a gradual decrease throughout the experiment. There were only minor differences between *C. elatum* and the controls in both crystallite width and percent crystallinity over the four time periods.

**Keywords:** X-ray diffraction, crystalline cellulose, wood decay, *Meruliporia incrassata*, *Chaetomium elatum*

## 1. INTRODUCTION

The degradation of wood by fungi has been studied intensely for many years due to its importance in both preservation of in-service wood and nutrient cycling in forests and other ecosystems. However, there remain many unanswered questions in this field, due at least in part to the difficulties associated with collecting and interpreting data about the biological processes of an organism growing in a material as complex as wood.

Wood cell walls are constructed of a matrix of cellulose, hemicelluloses, lignin, pectin, proteins, and other trace materials. Cellulose, which comprises 46-52% of the wood volume in softwoods and 39-52% in hardwoods (Zabel and Morrell 1992), is

composed of linear chains of  $\beta$ -1,4 linked D-anhydroglucopyranose, with cellobiose as the repeating unit (Fig. 1)(O'Sullivan 1997).

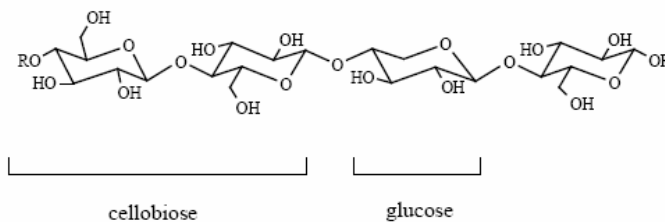


Figure 1: A schematic structure of a single cellulose chain (Maijala 2000).

A single chain of cellulose can be composed of up to 10,000 glucose subunits (Zabel and Morrell 1992). These chains are arranged in microfibrils, which are parallel groups of about 36 cellulose chains (Delmer and Armor 1995) that are wound around the wood cell at an angle more or less aligned with the fiber axis (Zabel and Morrell 1992, O'Sullivan 1997, Daniel 2003). The microfibrils consist of 60-70% crystalline cellulose and 30-40% amorphous cellulose surrounded by a hemicellulose and lignin matrix (Hermans and Weidinger 1949, Thygesen et al. 2005). The crystalline portions are formed when the cellulose chains that comprise the microfibril are so close together they form hydrogen bonds, creating a regularly patterned structure (O'Sullivan 1997). Studies have shown these crystalline regions are roughly 30Å across and 300 Å long (Fig. 2) (Thygesen et al. 2005). Approximately 30% of wood weight is cellulose in its crystalline form (Andersson et al. 2003). The amorphous portions of the microfibril, which lack the hydrogen bonding and regular structure found in their crystalline counterparts, are thought to separate these cellulose crystallites.

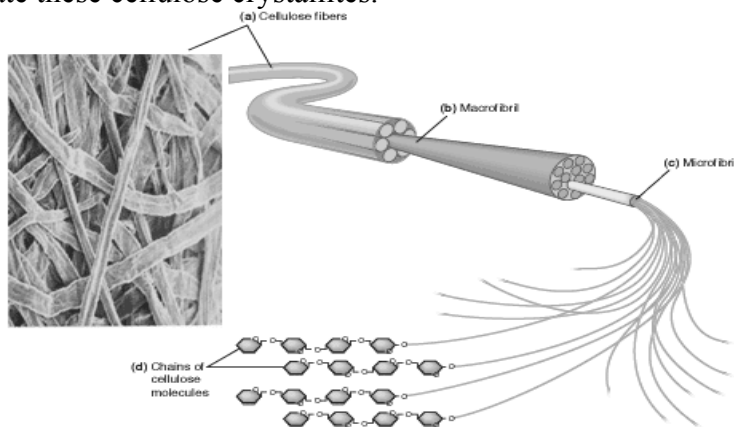


Figure 2: The structure of cellulose fibers (Insel 2006).

Crystalline cellulose is one of the more recalcitrant materials in wood and the ability to break apart these structures has evolved only in the wood decay fungi and some bacteria (Daniel 2003). Changes in wood crystallinity during decay can be used as a partial indicator of the effectiveness of these organisms.

X-ray diffraction (XRD), which detects the interference pattern created when x-rays encounter the regularly spaced crystalline cellulose planes in wood, has been used for decades as a rapid, non-destructive method for observing the crystalline portion of

wood, and is one of the primary tools used in the determination of the conformation and structure of cellulose microfibrils (Cullity 1978, Cave 1997, Lichtenegger et al. 1999).

The interference pattern created by the crystalline cellulose is used to determine the distance between the crystalline planes, the width of the microfibrils, and the overall percent of the wood that is in a crystalline state. The distance between the crystal planes can be determined by Eq. 1:

$$d \sin \theta = \lambda m \tag{1}$$

where **d** represents the distance between the crystal planes, **θ** (theta) is the angle between the plane and the diffracted or incident beam (Fig. 3), **λ** is the wavelength of the x rays, and **m** is an integer. The crystal planes are numbered according to the shortest vector required to get to any point in the crystal, in this case any glucose subunit (Ashcroft and Mermin 1976). In the literature different notations are often used for these vectors, therefore for cellulose crystals it should be noted that the (200), (020) and (002) planes are equivalent (Wada et al. 1997).

The width of the cellulose crystallite ( $X_c$ ) can be calculated using the Scherrer formula (Eq. 2):

$$X_s = (0.9\lambda)/(FWHM \cos \theta) \tag{2}$$

FWHM (full width at half maximum) represents the width of the peak at half the maximum height in radians (Figure 5). Theta (**θ**) represents the Bragg angle, which is half the 2θ value at the height of the peaks in the θ -2θ scan (Fig 4, 5). Lambda (**λ**) is the wavelength of the x-ray in angstroms (Å). All angles are in radians.

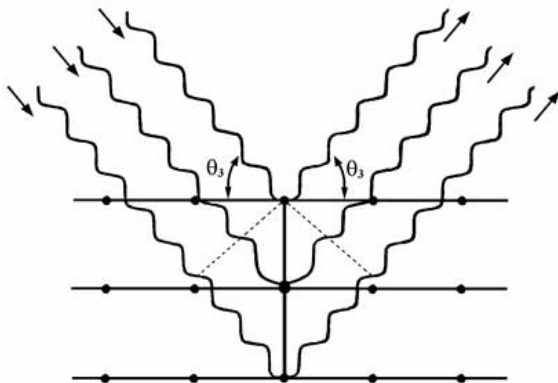


Figure 3: A representation of the the diffraction of x-rays from parallel planes(Scholotz and Uhlig 2006)

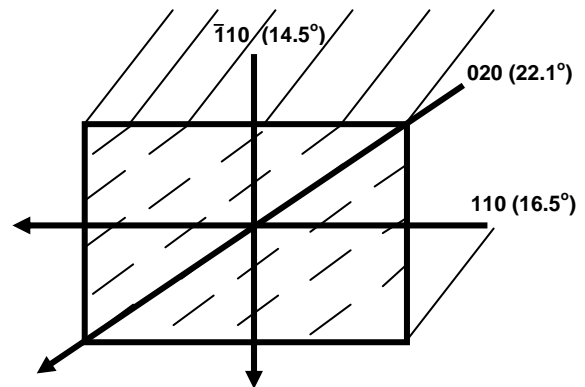


Figure 4: A top view of a cellulose microfibril (left) with corresponding crystal planes and 2θ values illustrated; 14.5°, 16.5°, and 22.1°, respectively (O'Sullivan 1997, Koyama 1997).

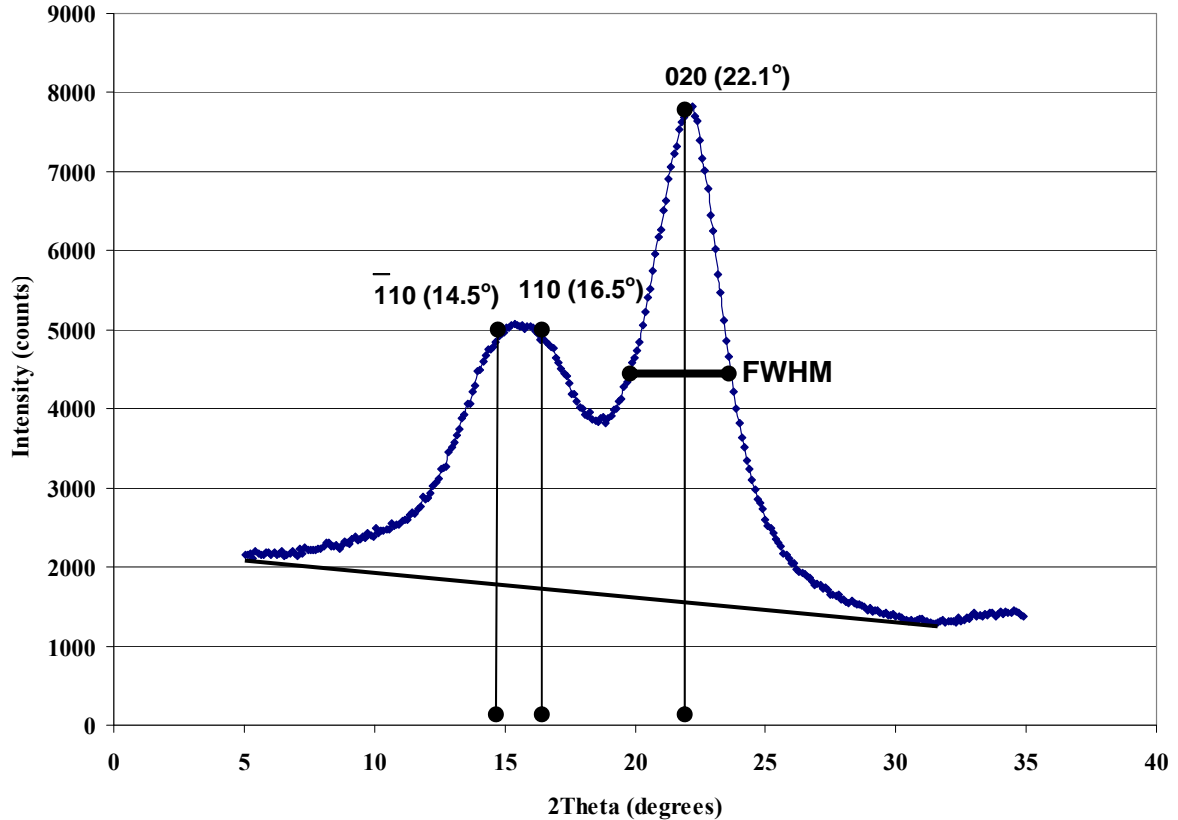


Figure 5:  $\theta$ - $2\theta$  scan of wood. The largest peak at approximately  $22^\circ$  represents the 002 plane, with the smaller peak representing the merger of the  $\bar{1}10$  and 110 planes at approximately  $14.5^\circ$  and  $16.5^\circ$ , respectively.

Brown rot fungi decay crystalline cellulose through a combination of non-enzymatic mechanisms and endo-acting cellulases (Maijala 2000). Classical endoglucanases split the cellulose internally, thus generating new free ends in the polymer. In white rot fungi, the process of digesting the cellulose polymer is completed by the actions of cellobiohydrolases (exoglucanases). These enzymes act from the free ends of the cellulose chains, releasing soluble cellobiose molecules which are subsequently hydrolyzed to absorbable glucose by  $\beta$ -glucosidases (Beguin and Aubert 1994).

*Coniophora puteana* is the only brown rot where exocellulases have been detected (Schmidhalter and Canecascini, 1993). It is thought, therefore, that degradation of the cellulose chains by brown rot fungi is catalyzed by the low molecular weight compounds and hydroxyl radicals these fungi are known to produce (Koenings, 1974, Rättö et al. 1997). Because production of these catalytic compounds is random, they may not be the only other factor enabling thorough degradation of wood cellulose by brown rot fungi (Cohen et al. 2005).

A number of studies have been conducted on the modification of crystalline cellulose by both brown and white rot wood decay fungi. Those focusing on the depolymerization of cellulose by the brown rot fungus *Postia placenta* have shown that early in the decay process this fungus will preferentially degrade the amorphous regions

of the cellulose microfibrils, temporarily increasing the overall crystallinity and the size of the crystallites (Highley et al. 1988, Klemen-Leyer et al. 1992).

Conversely, simultaneous white rot fungi will decrease the crystalline and amorphous portions of the wood at the same rate, resulting in a relatively slow reduction in crystallinity and size of the crystallites (Ohkoshi 1999).

Soft rot fungi belong to the families Ascomycota and Deuteromycota. These organisms grow within the cell walls of wood in contact with excessive moisture, causing cavities along the microfibrils in the S2 layer (Eriksson et al. 1990). While not classified with other decay fungi, they do cause strength loss and eventual weight loss in wood.

Colonization of wood by Type I soft rot fungi such as *Chaetomium elatum* occurs through the rays and, in the case of hardwoods, vessels. From here, the fungus moves into the wood cell lumen. In the initial stages of decay Type I soft rot will produce proboscis hyphae that penetrate the S3 layer and move into the S2 layer. Once there, these hyphae will align their growth parallel to the microfibrils, forming either a unidirectional hypha (L-bending hypha), or a T-shaped branch with hyphae projecting in opposite directions. The hyphae will continue to grow along the microfibrils, periodically secreting enzymes which produce the cavities that characterize Type I soft rot (Zainal 1978, Zabell and Morrell 1992). Eventually this continual creation of new cavities and the widening of old cavities will completely dissolve the S2 layer (Eriksson, 1990, Daniel 2003).

There is currently no published x-ray diffraction data describing the effects of soft rot fungi on cellulose crystallinity and crystallite size. The purpose of this study was to measure variations in percent crystallinity and crystalline size during degradation by two types of decay fungi. Creating enhanced understanding of the changes in cellulose crystallinity and the mechanisms of wood decay through the development of x-ray diffraction techniques may facilitate the development of more effective decay prevention measures.

## **2. MATERIALS AND METHODS**

### **2.1 Growth Conditions**

Fungi were maintained at 21°C on 2% (w/v) Potato Dextrose Agar (PDA) until inoculation. Fungi used in this study were *Meruliporia incrassata* (Berk. & M.A. Curtis) Murrill, mfstoner-1 was collected from decaying wood in California by Dr. M.F. Stoner, and *Chaetomium elatum* (Kunze), ATCC 38799 purchased from the American Type Culture Collection.

### **2.2 Soil Block Assays**

Four 1cm<sup>2</sup> pieces of inoculum were taken from the outer edge of mycelium of 3 week old fungal colonies and placed into modified AWPA soil block jars (AWPA 2003). Each piece of inoculum was placed at one corner of a set of birch feeder strips, on top of approximately one cup of a 1:1:1 mixture of potting soil, sphagnum peat moss and horticultural grade vermiculite, hydrated with deionized water.

One 1.2 x 2.5 x 2.5 cm transverse spruce block was placed in the jar after the mycelial mat had covered the set of birch feeder strips. Fungi were allowed to grow for 2,

4, 6 and 8 weeks after the addition of the wood block. There were 5 replicates per fungus per harvest, as well as 5 uninoculated controls.

### 2.3 Processing and X-Ray Diffraction Analysis

All blocks and powders were dried and weighed immediately after harvest. Blocks were ground in a Wiley Mill and passed through a standard 40 mesh screen (420 $\mu$ m). All powders were pressed manually using a Dake Press (Dake, Grand Falls, MI) into cylindrical wafers 2cm in diameter and 0.3-0.5 cm thick. Thickness of the pellets was not tightly controlled because pellet thickness increases the overall intensity of the scan and not the resulting peak shapes or heights when compared to the baseline.

Wood wafers were scanned using a Panalytical X'Pert X-Ray diffraction machine with symmetric  $\theta$ - $2\theta$  Bragg-Brentano scattering geometry (Panalytical, Netherlands). Nickel filtered  $K\alpha$  radiation with a wavelength of 1.542 $\text{\AA}$  was used to perform  $\theta$ - $2\theta$  scans. The incident beam was passed through a fixed divergence slit of  $1/16^\circ$  and an anti-scatter slit of  $1/8^\circ$ , as well as a 15mm mask. The diffracted beam was passed through a 5.0 anti-scatter slit. Data were collected in the  $2\theta$ -range  $5$ - $35^\circ$  with a step size of  $0.01^\circ$ . The scans proceeded at  $0.08^\circ$  per second (150 seconds per step).

### 2.4 Determination of Crystallite Width and Sample Crystallinity

Spectra were deconvoluted into their constituent peaks using the Profile Fit program (PW3205, PANalytical B.V., Netherlands, 1999, version 1.0C). A program designed to deconvolute powder diffraction spectra into their constituent Bragg reflections by fitting analytically derived peaks to measured scans. Variations in the crystallinity index between the samples were controlled for by scanning five control samples per harvest period and averaging the spectra.

Initial values for the first two peaks derived from cellulose I were set at  $2\theta = 14.5^\circ$  ( $\bar{1}10$ ) and  $16.5^\circ$  (110), the average values found in the literature for softwoods (Andersson et al. 2003, Newman 2004, Borysiak and Doczekalska 2005, Thygesen et al 2005). Organosolv lignin (Sigma-Aldrich Co., Chicago, IL, USA) was chosen as an amorphous standard (O'Sullivan 1997, Thygesen et al 2005). This material was pressed into a pellet and scanned, then fitted with a Pseudo-Voigt peak. The amorphous peak was added to the computer program along with the initial estimates of the crystalline peaks. The program was allowed to refine the  $2\theta$  values and FWHM values for the crystalline peaks, and the intensities of both the crystalline and amorphous peaks.

Deconvoluted peaks were analyzed to determine the average micelle crystallite width of the cellulose microcrystals. Overall percent crystallinity, which is defined as the ratio of crystalline cellulose to the total amount of sample material, was also calculated using Eq. 2.

Percent crystallinity in the sample was calculated by multiplying the non-overlapping areas of peaks from plane  $\bar{1}10$ , 110 and 002 by the total area of the crystalline peaks and the amorphous standard.

The crystallite width calculated with the Eq. 2 is influenced by the FWHM of the peak generated from the 002-plane. The center of the peak was found to vary by  $\pm 0.1$  degrees thus slightly changing the FWHM and affecting the crystallite width and the standard deviation. A  $2\theta$ -average value was calculated for the peak of the 002-plane.

## 2.5 Statistics

Statistical analysis of weight loss, crystallite width, and percent crystallinity values were done using one way ANOVA tests calculated by SySTAT v.11 (Systat Software Inc., San Jose, California, USA,) and protected Fisher LSD. Standard deviation for the 5 replicates was calculated.

## 3. RESULTS

### 3.1 Weight Loss

The inoculated blocks with *M. incrassata* and *C. elatum* all showed heavy, mycelia growth at 8 weeks of incubation (Fig. 6, 7, and 8).



Figure 6: Wood block inoculated with *M. incrassata*, week 8.



Figure 7: Wood block inoculated with *C. elatum*, week 8.



Figure 8: Uninoculated wood block, week 8.



Weight loss results show a steady decay by *M. incrassata* over all 8 weeks, up to a maximum of 46%. The blocks incubated with *C. elatum* show no significant weight loss compared to the controls ( $P = 0.839$  to  $0.932$ ) (Fig. 9).

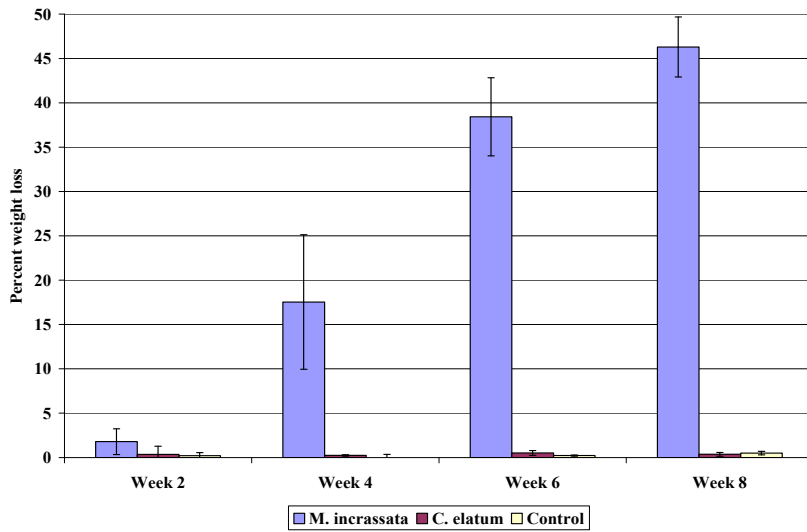


Figure 9: Week 2, 4, 6 and 8 average measured weight losses for wood blocks inoculated with *M. incrassata* and *C. elatum*, and uninoculated blocks ( $n = 5$ ). Bars represent standard deviation.

### 3.2 Raw Scans

Scans show a reasonable variability in the control, ranging from a minimum value of 7500 counts for the 002 plane (peak at  $\sim 22^\circ$ ) at Week 6 to a maximum of approximately 9000 counts at Week 4 (Data not shown). For the first three harvest periods the raw scans show a gradual decrease in cellulose crystallinity (Data not shown), with a notable difference in peak height and shape at Week 8 (Fig. 10).

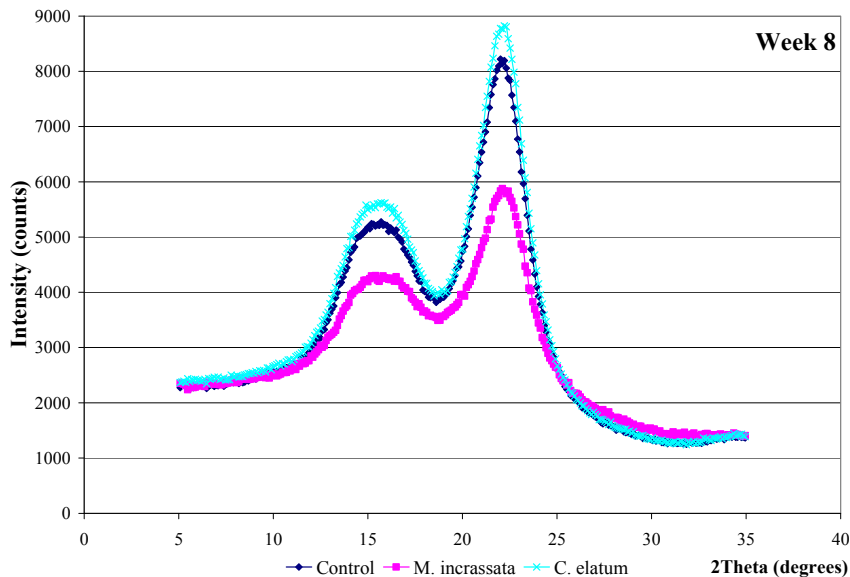


Figure 10: Raw X-ray diffraction patterns for compiled scans of wood degraded by *M. incrassata* at 8 weeks of decay,  $n = 5$ .

Examples of peaks deconvoluted with Profile Fit are presented in Figure 11 and Figure 12, showing the reflection pattern of crystalline cellulose in the 2θ-range 5-35° with the peaks presented as Pseudo-Voigt functions. The intensity of the amorphous peak was adjusted according to the results found in the raw scans to compensate for variation and decay of the wood block.

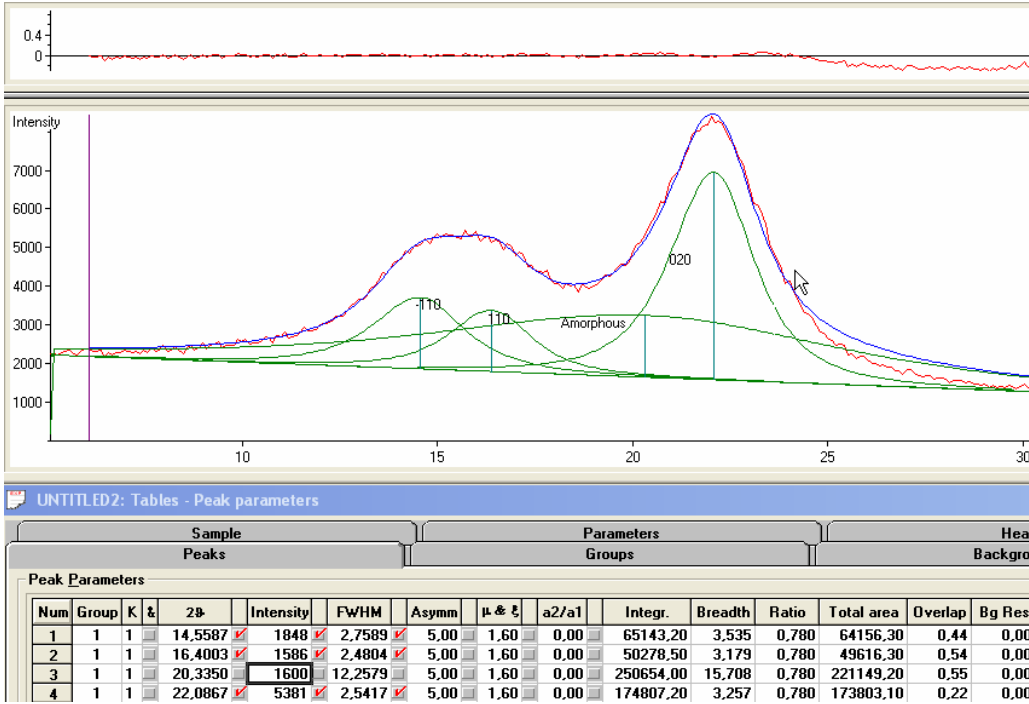


Figure 11: Profile fit deconvoluted  $\theta$ - $2\theta$  scan of control wood block after 2 weeks of incubation. The red line above the spectrum shows how well the peaks fit the curve.

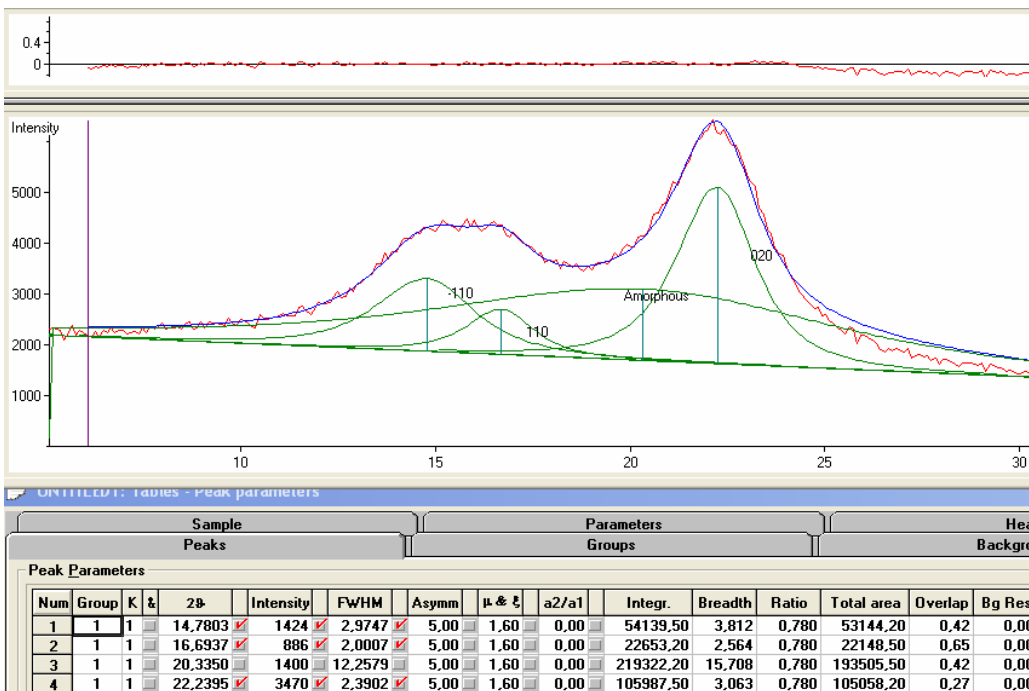


Figure 12: Profile fit deconvoluted  $\theta$ -2 $\theta$  scan of wood block inoculated with *M. incrassata* for 8 weeks. The red line above the spectrum shows how well the peaks fit the curve.

### 3.3 Crystallite Width

The controls showed no significant difference in crystal width during the 8 weeks of incubation ( $P = 0.630$ ).

The values for crystallite width showed no significant differences between the controls and *C. elatum* for any of the harvest periods, however at week 8 crystallite size was appearing to increase slowly ( $P > 0.062$ ) (Fig. 13).

At week 4, *M. incrassata* showed a significant increase in crystallite width from week 2 relative to the control ( $P = 0.03$ ). Comparisons between Week 4 and Week 8 and Week 6 and Week 8 both showed a significant decrease in the crystallite width of the wood incubated by *M. incrassata* ( $P = 0.001$  and  $P = 0.035$ , respectively). Further the decrease in crystallite width by Week 8 was not significant compared to the controls ( $P = 0.467$ ) (Fig. 13).

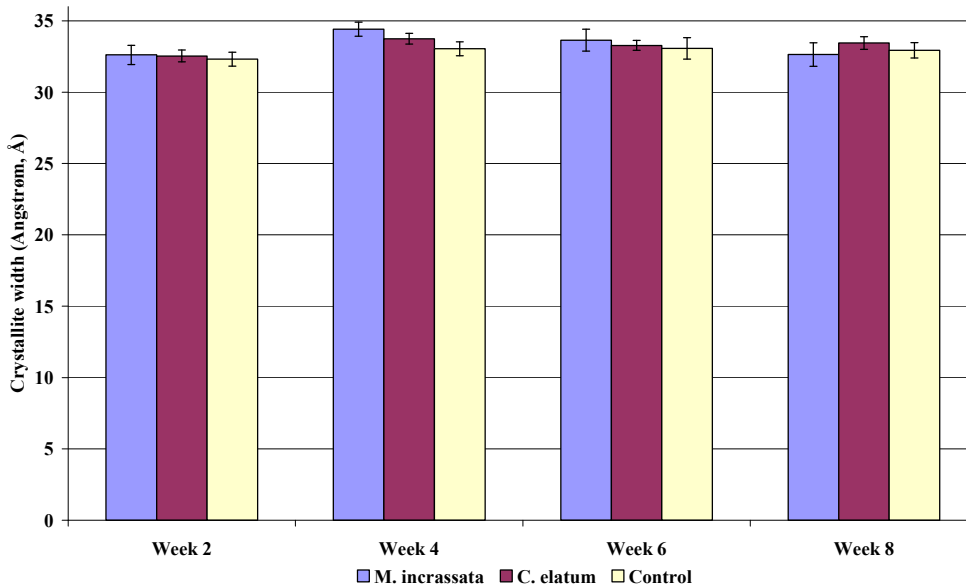


Figure 13: Crystallite width in wood inoculated with *M. incrassata*, *C. elatum*, and in uninoculated blocks at 2, 4, 6, and 8 weeks of incubation. Bars represent standard deviation.

### 3.4 Percent Crystallinity

The percent crystallinity in the control blocks fluctuated between 37.0% ( $\pm 0.7$ ) and 41.5% ( $\pm 1.1$ ).

There was a significant increase in percent crystallinity from approximately 37% to 41% caused by *M. incrassata* by Week 2 ( $P = 0.005$ ). This was followed by a drop in Week 4 and Week 6 with a further, significant decline in percent crystallinity to 29.1% by Week 8 ( $P = 0.000$ ) (Fig. 14).

For *C. elatum* there was no significant change in percent crystallinity over the 8 weeks of incubation in comparison to the control group, however the percent crystallinity did seem to increase at Week 2 relative to the control ( $P = 0.092$ ).

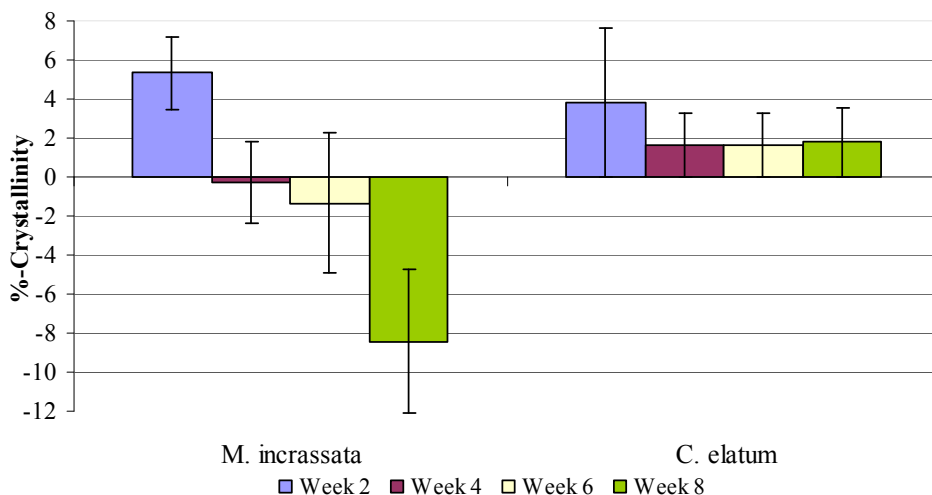


Figure 14: Changes in percent crystallinity in wood inoculated with *M. incrassata* and the control blocks, and *C. elatum* and the control blocks, respectively. Bars represent standard deviation.

#### 4. DISCUSSION

The interference patterns produced by X-ray diffraction of degraded wood powders are useful in characterizing the crystalline cellulose structure of wood substrates. However, when analyzing the crystallinity in wood, the presence of significant amounts of amorphous material can cause x-ray scattering and result in broad, overlapping peaks which are difficult to distinguish from one another (Thygesen et al. 2005). Separating the amorphous regions from the pure crystalline images in a diffraction pattern is a challenge and can make accurate interpretation of XRD results difficult.

Well crystallized samples, such as sodium chloride, give sharp diffraction peaks which are easily separated from the amorphous background (Ashcroft and Mermin 1976). With cellulose crystals in wood, however, one must make assumptions about the size, shape, and spacing of the crystallites, as well as the overall shape and size of the amorphous cellulose, hemicelluloses and lignin. When evaluating the cellulose crystallinity it is important to select a method that takes into account the peak overlap and the broadened diffraction peaks to get a reliable determination of the sample crystallinity.

There are other factors that may also broaden the diffracted beam and result in skewed peaks (Cullity 1978). These include the small size of cellulose crystallites (typically 20-50Å in diameter) (Thygesen et al. 2005), the alignment of crystals in the microfibrils which may not conform perfectly to other microfibrils within the same macrofibril or between the microfibrils in the three layers of the secondary cell wall, (S1, S2, S3) (Cave 1997), the random arrangement of cellulose microfibrils in the primary wall (Bhatnagar and Sain, 2005), and finally a disruption of the crystalline matrix by grinding of wood samples.

Interpreting data obtained from X-ray diffraction spectra requires consideration of the deconvolution method employed and the assumptions made. A number of investigators have studied the differences between spectra deconvoluted with different deconvolution programs and methods (Thygesen et al. 2005, Wada et al. 1997). We

discovered that altering our assumptions slightly had a significant impact on the data output using ProFit alone.

During the course of these experiments, we used four different deconvolution methods ranging from allowing the computer nearly complete freedom in adjusting peak locations (20 values), heights, and FWHM values to setting all parameters for the amorphous peak and allowing refinement only of the crystalline peaks. All methods affected both comparative values and standard deviations for crystallite width and percent crystallinity.

Thygesen et al. (2005) did a comparison on different methods for determination of crystallinity and cellulose content and found that there was a significant variation amongst them and that some were preferable for certain studies. Therefore the choice of method for the deconvolution of data should be considered carefully. Our final data was calculated by setting the location and FWHM value for the amorphous peak based on our amorphous standard, while allowing for adjustment of the intensity by the ProFit program. This facilitated creation of a standard shape for the amorphous peak and allowed us to attribute changes in the amount of amorphous material in the wood substrate to the fungi.

The crystallite width of  $33 \pm 1.5 \text{ \AA}$  calculated for the control wood blocks in this study were within the range of results from recent publications (Andersson et al. 2003, Newman 2004, Thygesen et al. 2005,). They found it to be  $31 \pm 1 \text{ \AA}$ ,  $30\text{-}34 \text{ \AA}$ , and  $33.4 (\pm 0.4)$ , respectively. The slight variation between these and the results from this study could be due to the experimental approach with the instrument and the process of deconvolution.

In the literature, crystallinity in wood is presented either as degree of crystallinity or percent crystallinity. The term ‘degree of crystallinity’ has been used by Borysiak and Doczekalska (2005) and others to express the ratio of cellulose that is in the crystalline form (~70%). Percent crystallinity, on the other hand, is a ratio of the amount of crystalline cellulose compared to the total amount of material in the wood. Approximately 30% of wood weight is cellulose in its crystalline form (Andersson et al. 2003, Thygesen et al 2005). In this study the percent crystallinity was calculated, as it was not possible to separate out and independently measure the crystallinity of only the cellulose portions of the wood.

While modifications of the crystalline structure of the wood substrate by *M. incrassata* were detectable throughout the 8-week study period, it should be noted that the results represent the average crystallite width and crystallinity throughout the entire block of wood. Because fungal degradation is a dynamic process occurring along the length of any given hypha as it progresses into the wood, relatively small overall differences were found when reviewing the general changes for the entire wood block.

The significant increase in percent crystallinity for *M. incrassata* at Week 2 may be due to the initial degradation of the easily accessible materials stored in the rays and a preferential attack on the amorphous cellulose early in the decay process (Klemen-Leyer et al. 1992). At Week 2, the crystallite width is the same as in the controls, possibly because the fungus has not yet penetrated the other materials in the wood cell walls that cover the crystalline structure. At Week 4, the weight loss is significant ( $17.5\% \pm 7.2$ ), while the percent crystallinity has returned to the level of the controls, and the crystallite size has increased compared to the controls. This could be the result of the initial degradation of the amorphous hemicelluloses and widening of the crystallites by non-enzymatic mechanisms, such as hydroxyl radicals. These non-enzymatic processes

increase the amount of amorphous material present in the wood (Cohen et al. 2005, Klemen-Leyer et al. 1992).

Crystallite width has decreased by Week 8 possibly due to enzymatic decay, which breaks down and allows for absorption of the outer amorphous edges of the cellulose crystals by the fungi. Percent crystallinity values are also decreasing, yet at a slower rate. This is due to the fungi accumulating these amorphous polysaccharide fragments faster than they are degraded (Klemen-Leyer 1992). An average weight loss of  $46.3\% \pm 4.3$  indicates that the wood blocks are fairly well decayed as maximum decay would be  $\sim 75\%$  (Zabel and Morrell 1992).

By Week 8 most of the cellulose crystals have been attacked by the fungi, and are now being depolymerized and absorbed by the fungi. Percent crystallinity values for *M. incrassata* at Week 8 are significantly lower than the controls as the remaining undigested crystallites continue to be broken apart. In an experiment of longer duration, we would likely see a continued decrease in both percent crystallinity and crystallite size as the fungi continue to degrade the cellulose structure of the wood.

Results from wood blocks incubated with *C. elatum* show no significant weight loss but indicate a slight overall increase in percent crystallinity ( $P = 0.107$ ), which may be due to slight degradation of the amorphous portions of the wood. It is not surprising, however, that these results are not significant at the  $P = 0.05$  level, as soft rot fungi alter only the outer portion of the wood (Zabel and Morrell 1992) and these changes are undetectable when measuring overall percent crystallinity within the wood block. A longer incubation period would have possibly yielded a greater decrease in the percent wood crystallinity. Further study has begun to determine the validity of this assumption.

## 5. CONCLUSIONS

When used to calculate cellulose crystallinity in wood, X-ray diffraction can also be used as a measure of the efficiency of wood decay fungi. However, results must be evaluated with caution to account for the influence of amorphous materials in the wood samples and the small crystallite sizes.

Results from this study show that there is a significant decrease in crystallinity in wood samples inoculated with *M. incrassata* after 8 weeks. The crystallite size temporarily increased at four weeks of incubation. There were no significant changes in the crystalline wood structure of samples inoculated with *C. elatum*, although a slight increase in percent crystallinity was observed.

Further study, of longer duration, will lead to increased knowledge of degradative pathways and creation of increasingly more effective decay prevention measures.

## 6. ACKNOWLEDGMENTS

We would like to thank Joan Perkins, Jason Oliver, Dr. David Frankel and Dr. George Bernhardt for their invaluable technical and editorial assistance.

## 7. REFERENCES

- Andersson S, Serimaa R, Paakkari T, Saranpää P, Pesonen E (2003): Crystallinity of wood and the size of cellulose crystallites in Norway spruce (*Picea abies*). *Journal of wood science*, **49**, 531-537.
- Ashcroft NW, Mermin ND (1976): *Solid state physics*, Holt, Rinehart and Winston, NY, USA. pp 65-128.
- AWPA (2003) Standard method of testing wood preservatives by laboratory soil-block cultures. In *Book of Standards*. pp. 206-212. American Wood Preservers' Association, Granbury, TX, USA.
- Beguín P, Aubert J P (1994): The biological degradation of cellulose. *FEMS Microbiological Review*, **13**, 25–58.
- Bhatnagar A, Sain M (2005): Processing of cellulose nanofiber-reinforced composites. *Journal of reinforced plastics and composites*, **24**(12), 1259-1268.
- Borysiak S, Doczekalska B (2005): X-ray diffraction study of the pine wood treated with NaOH. *Fibres & Textiles in Eastern Europe*, **13**(5), 87-89.
- Cave I D (1997): Theory of X-ray measurement of microfibril angle in wood. *Wood Science and Technology*, **31**, 143-152.
- Cohen, R., Suzuki M R, Hammel K E (2005): Processive endoglucanase active in crystalline cellulose hydrolysis by the brown rot basidiomycete *Gloeophyllum trabeum*. *Applied and Environmental Microbiology*, **71**(5), 2412–2417.
- Cullity B D (1978): *Elements of x-ray diffraction*. 2<sup>nd</sup> Addison-Wesley Publishing company, Inc. Reading, Massachusetts, USA, pp 81-105.
- Daniel G (2003): Microview of wood under degradation by bacteria and fungi. In: *Wood Degradation and Preservation: Advances in Our Changing World*. pp 34-72. Eds. Goodell B, Nicholas D D, Schultz T P, American Chemical Society, Washington D.C., USA.
- Delmer D P, Armor, Y (1995): Cellulose biosynthesis. *Plant Cell*, **7**, 987-1000.
- Eriksson K E L, Blanchette R A, Ander P (1990): Microbial and enzymatic degradation of wood and wood components, Springer-Verlag, Berlin, Germany, pp 56-72.
- Hermans P H, Weidinger A (1949): X-ray studies on the crystallinity of cellulose. *Journal of Polymer Science*, **4**(2), 135 – 144.
- Highley T, Ibach R, Kirk T K (1988) Properties of cellulose degraded by the brown rot fungus, *Postia placenta*. *International Research Group on Wood preservation*, IRG/WP/1350.

- Insel P, Turner R E, Ross D (2006): Discovering Nutrition. 2<sup>nd</sup> edition. <http://nutrition.jbpub.com/discovering/2e/index.cfm>. Retrieved 20.March 2007.
- Klemen-Leyer K, Agosin E, Conner A H, Kirk T K (1992): Changes in the molecular size distribution of cellulose during attack by white and brown rot fungi. *Applied and Environmental Microbiology*, **58**, 1266-1270.
- Koenings J W (1974): Hydrogen peroxide and iron: a proposed system for decomposition of wood by brown-rot Basidiomycetes. *Wood and Fiber science*, **6**, 66-80.
- Koyama M, Helbert W, Imai T, Sugiyama J, Henrissat B (1997): Parallel-up structure evidences the molecular directionality during biosynthesis of bacterial cellulose. *Proceedings of the National Academy of Sciences USA*, **94**, 9091-9095.
- Lichtenegger H, Müller M, Paris O, Riekkel C, Fratzl P (1999): Imaging of the helical arrangement of cellulose fibrils in wood by synchrotron X-ray microdiffraction. *Journal of Applied Crystallography*, **32**, 1127-1133.
- Maijala P (2000): Heterobasidion annosum and wood decay: Enzymology of cellulose, hemicellulose, and lignin degradation. *Academic dissertation*. HU-P-D135, University of Helsinki, Finland.
- Newman R H (2004): Homogeneity in cellulose crystallinity between samples of *Pinus radiata* wood. *Holzforschung*, **58**, 91-96.
- Ohkoshi M, Kato A, Suzuki K, Hayashi N, Ishihara M (1999): Characterization of acetylated wood decayed by brown-rot and white-rot fungi. *Journal of Wood Science* **45**, 69-75.
- O'Sullivan A C (1997): Cellulose: the structure slowly unravels. *Cellulose* **4**, 173-207.
- Rättö M, Ritschkoff A-C, Viikari L (1997): The effect of oxidative pretreatment on cellulose degradation by *Postia placenta* and *Trichoderma reesei* cellulases, **48**, 53-57.
- Schlotz R, Uhlig S (2006): Introduction to X-ray Fluorescence Analysis (XRF). [http://www.bruker-nonius.com/fileadmin/user\\_upload/xrfintro/author.html](http://www.bruker-nonius.com/fileadmin/user_upload/xrfintro/author.html). Retrieved 23. March 2007.
- Schmidhalter D R, Canevascini G (1993): Purification and characterization of two exocellobiohydrolases from the brown rot fungus *Coniophora puteana* (Schum ex Fr.) Karst. *Archives of Biochemistry and Biophysics*, **300**, 551-558.
- Thygesen A, Oddershede J, Lilholt H, Thomsen A B, Ståhl K (2005): On the determination of crystallinity and cellulose content in plant fibers. *Cellulose*, **12(6)**, 563-576.
- Wada M, Okano T, Sugiyama J (1997): Synchrotron-radiated X-ray and neutron diffraction study of native cellulose. *Cellulose*, **4**, 221-232.



Zabel R A, Morrell J J (1992): *Wood Microbiology: Decay and its prevention*. Academic Press, Inc. San Diego, pp. 21-194.

Zainal A S (1978): A new explanation for soft rot cavity formation in the S2 layer of wood cell walls. *Wood Science and Technology*, **12**, 105-110.